Vol. 43, No. 2 (2021) 247-258, DOI: 10.24874/ti.945.08.20.11

Tribology in Industry

www.tribology.rs

RESEARCH

Sliding Wear Investigation of Ni-based Coating for High-Temperature Application

S.W. Rukhande[a,b,*], W.S. Rathod[a], D. Bhosale[a]

[a]*Mechanical Engineering Department, Veermata Jijabai Technological Institute, Mumbai, India, 400019,*
[b]*Mechanical Engineering Department, Fr. C. Rodrigues Institute of Technology, Vashi, Navi Mumbai, India, 400703.*

Keywords:

NiCrBSiFe
Stainless steel 316L
Dry sliding wear
High temperature
High-velocity oxy-fuel

* Corresponding author:

Sanjay W. Rukhande
Email: Sanjay.rukhande@fcrit.ac.in

Received: 15 August 2020
Revised: 16 September 2020
Accepted: 18 November 2020

A B S T R A C T

*The effect of high temperature on the sliding wear and friction behaviour of NiCrBSiFe powder coating on stainless steel 316L substrate was investigated. The NiCrSiBFe coatings were obtained using a thermal spray technique. The sliding wear tests were performed as per ASTM G99 on the pin on disc tribometer from room temperature (28 °C) to 700 °C temperature condition. The coating characterization was carried out with X-ray diffraction, scanning electron microscopy, porosity analysis and nano-indentation. A 3D non-contact analysis was performed on the wear-track to obtain the wear rate of the coating at different temperatures. The coefficient of friction and wear rate was obtained for the coatings against silicon nitride (*1580 $HV_{0.3}$*) material. The coefficient of friction was obtained as 0.68, 0.15 and 0.51 at room temperature, 300 °C and 700 °C, respectively. The mild wear range confirms the efficacy of the coating at high temperature. The wear rate and coefficient of friction of the coatings were influenced by the oxidation and mechanical properties at the high-temperature conditions. The wear rate increases from 300 °C to 700 °C as the substantial amount of material loss from the coating surface occurred due to the coatings thermal softening and the fragmentation of oxides like CrO_3, SiO_2 and NiO.*

1. INTRODUCTION

The high-temperature wear and oxidation resistance are the basic requirements for any mechanical components serving in a high-temperature environment. The various coating materials and deposition methods applied to the surfaces of the mechanical parts to control the wear and oxidation. Recently, the study on the thermal spray powders and thermal spray methods attracted the researchers due to their extensive applications in the industries. The properties of the coatings are significantly differed due to the deposition process and alloying elements.

The self-fluxing powder NiCrBSi extensively used for the surface modification of the components subjected to the tribological conditions, due to high corrosion and wear re-

sistance [1,2]. The chromium phases improve high-temperature oxidation and wear resistance[3]. The self-fluxing properties improved due to silicon and boron elements in the powder. Some of the industrial applications of this coating are turbine blades, coal-fired boilers tube, heat exchangers, piston rings and agricultural machinery [4,5]. In some of the research, the NiCrBSi composite coating developed by different processes for high-temperature conditions. The process like laser remelting [6,7], laser cladding [8], pack cementation method [9], plasma spraying [10–12], HVOF [13–16] used for the deposition of the coating. The high-velocity oxy-fuel (HVOF) and atmospheric plasma spray (APS) processes are the extensively used thermal spraying methods for the NiCrBSi powder [17,18]. However, the HVOF process gained more acceptance due to portability and easier handling. Also, it is known for producing dense coatings with low oxide formation. The APS deposited NiCrBSi–graphite coatings show the minor effect on the erosion behaviour up to 650 °C [11]. The laser remelting composite coatings of NiCrBSi and WC on stainless steel shows the enhanced sliding wear performance up to 600 °C [19]. At temperature up to 750 °C, the HVOF sprayed WC-Cr_3C_2-Ni coating provide higher wear resistance for dry sliding conditions [20]. The HVOF deposited IN718-Al_2O_3 offers improved microhardness and high oxidation resistance [21].

The wear rates of the HVOF coated cast iron discs found negligible at 300 ℃[22]. The HVOF sprayed NiCrBSi coating has superb wear resistance at high temperature, and the wear rate inversely proportional to the load [23]. M. Kaur et al. [24] observed the superb wear resistance of the APS and HVOF sprayed NiCrBSi powder coatings on AISI H11 steel substrate against 20MnCr5 at room temperature and 400 ℃ However, the wear rate found upsurge considerably at 800 °C. The wear depends on the coating's microstructure at low temperature, whereas the oxide layer governs the wear at high-temperatures. The wear mechanism transforms from abrasive wear to adhesive and oxidation wear with increasing temperature [25,26]. The high-temperature oxidation prominently affects the sliding wears [27,28]. The wear behaviour of the coating depends on the substrate material chemical composition [29]. The hardness of the coating has a higher impact on the wear, but it is not sufficient to describe the wear completely. There is close association of the wear behaviour with the ratios H/E_r and H^3/E_r^2, known as elastic deformation resistance [18] and the yield pressure or the plastic deformation resistance of the coating surface [30], respectively. Where, H is the hardness of the coating surface and E_r is the reduced elasticity modulus. The deformation due to external forces on the contact material recovered elastically with a higher (H/E_r) ratio, similarly, higher the ratio (H^3/E_r^2) means higher the resistance to plastic deformation. The elastic recovery value (η) is the ratio of elastic deformation energy to the total deformation energy, signifies the energy released from the material surface, which is a measure for the surface subjected to impact loading. The wear resistance is directly proportional to the ratio (H/E_r), (H^3/E_r^2) and the recovery value (η) [31].

The feedstock powder and substrate material having close values of coefficient of thermal expansion produces the coating with enhanced wear resistive properties. The stainless steel 316L has excellent corrosion resistance and deformability, hence widely used in biomedical implants, the nuclear power plants and petrochemical industries. But, due to its low hardness, it has poor wear resistance which reduces service life and limits its applications. Thus it is of importance to improve the wear resistance of stainless steel 316L with surface modification. From the literature, it is observed that very few tries have been made for investigating the NiCrBSiFe coating wear at the high-temperature condition. However, the high-temperature wear performance of NiCrBSiFe coatings on stainless steel 316L substrate has not studied yet. The proposed study will aid to understand the sliding wear and friction phenomenon of HVOF sprayed NiCrBSiFe coating on stainless steel 316L substrate at high-temperature up to 700 ℃

The main objective of this work is to examine the coating performance for unidirectional sliding wear at an elevated temperature up to 700 ℃ The microstructure and the mechanical properties of the Ni-based coatings are studied. The endurance capability of the coating is determined using the nano-indentation. The wear mechanism occurred at room temperature and high-temperatures, are examined.

2. EXPERIMENTAL

2.1 Coating preparation

The stainless steel 316L grade was used as a substrate material having a chemical composition of C - 0.018 %, Mn -1.3 %, Si – 0.36 %, Cr – 16.62 %, Mo – 2.07 %, P – 0.0032 %, S – 0.003 % and Ni – 10.12 %. The feedstock powder NiCrSiBFe, available with PAC, Cincinnati, Ohio was used for the deposition. The nickel-based powder composed of chromium (14.5 %), boron (3.2 %), silicon (4.5 %), iron (4.5 %), and nickel (73.3 %). The particles size variation in the NiCrSiBFe powder was determined by particle size analysis. The powder particles have a mean size of 28.7 μm.

Table 1. The coating processing parameters.

Process parameter	Values
The oxygen gas pressure	10 bar
Fuel (LPG) pressure	7 bar
Gas flow rate	240 SLPM (Oxygen), 550 SLPM (Air)
The powder feed rate	45 g/min
Average particle velocity	534 m/s
The avg. particle temperature	2210 ^{o}C
The stand-off distance	150 mm
The deposition efficiency	65 %

The specimens were grit blasted by alumina 20 Mesh (Virgin Grade) to achieve enough surface roughness which promotes the mechanical bonding of the sprayed particles and substrate. The blasting was carried out from 150 mm distance with the 90° angles at 0.5 Mpa air pressure. The HIPOJET-2700 gun used for the powder deposition by the HVOF process. The oxygen and liquid petroleum gas (LPG) pressure were maintained at 10 bar and 7 bar, respectively. The oxygen and airflow rates were kept at 240 SLPM (standard litres per minutes) and 550 SLPM, respectively. The HVOF spraying parameters used for obtaining the coating are shown in Table 1.

2.2 Coating characterization

The coating microstructures and worn track surfaces examined using Carl Zeiss (Gemini FE-SEM 300) scanning electron microscope. The secondary electron images were obtained at 500X magnification for the coating surface and cross-section. The coating thickness was measured from the cross-section SEM image. The Empyrean diffractometer used for the phase identification in the powder and coatings. The XRD analysis performed with Cu Kα (1.54060Å) radiation over an angular range of 20°≤ 2θ≤ 90° and a step size of 0.02°. The generator maintained at 45 kV voltage and 40 mA current. The porosity measured at a different position on the coating cross-section to measure the pores volume fraction. An image thresholding technique used for porosity measurement in the ImageJ software. The nano-indentation test was carried out with a load of 9 mN for 10 seconds with Hysitron and Bruker Inc. nano indentor. A standard diamond Berkovich indentor having hardness value 1140 GPa and poison's ratio of 0.07 was used to perform indentation test. Ten indentations performed along the coating cross-section diagonally and the average obtained for elasticity modulus and nano hardness. The (H/E_r) ratio, (H^3/E_r^2) and the recovery value (η) were determined for the coating. The as-sprayed coating roughness determined by taking an average of ten readings.

2.3 Tribological testing at high temperature

The disc of 8 mm thickness and 40 mm diameter was prepared from the HVOF sprayed NiCrBSiFe coating using EDM operation. The surface roughness was achieved on the disc up to 0.3 μm by polishing the disc with graded paper and diamond paste. The silicon nitride balls of 10 mm diameter having **1580 $HV_{0.3}$** hardness were used as a counter material for the experimentation. A (TR-20LE, CHM-800) Ducom made tribometer was used for the sliding wear experimentation at different temperature condition. Before the test, the coating disc and the counter ball were cleaned with ethanol. ASTM G99 standard procedure was followed to perform the series of experiments. The experiments were performed at 0.3 m/s sliding velocity, 10 N load at the room temperature, 300, 500 and 700 °C. The wear depth and the frictional forces were recorded and analysed. From EDAX analysis, the weight percentage of the elements present on the wear-track surface were determined. The volumetric wear loss, and wear rate (mm^3/N.m) were obtained with 3D non-contact analysis, using the Alicona microscope. All the wear tracks on the coatings correspond to room temperature, 300, 500 and 700 °C were analysed,

and the depth profiles obtained for all the wear tracks. The area under the curve was measured using the integration method to get the wear-track cross-sectional area.

The volume loss was determined using equation, $V=A\times 2\pi R$, Where, V- a volume of the wear-track in mm^3, A - a cross-section area of the wear-track in mm^2, and R - wear-track radius in mm. The wear rate determined from the load (P), sliding distance (S), and the volume loss (V) as mentioned in equation, wear rate = V/ (P×S). The specific volumetric wear rates were determined and compared at different temperatures.

3. RESULT AND DISCUSSION

3.1 Characterization

Figure 1 shows the XRD pattern of powder and HVOF sprayed coating obtained by X-ray diffraction analysis. High-intensity phases of Ni and Cr_3Si were noted at 44.3° diffraction angle. The medium peaks were observed for $Ni_{31}Si_{12}$ and Ni_2B. The low-intensity CrB phase was also detected for the powder and coating.

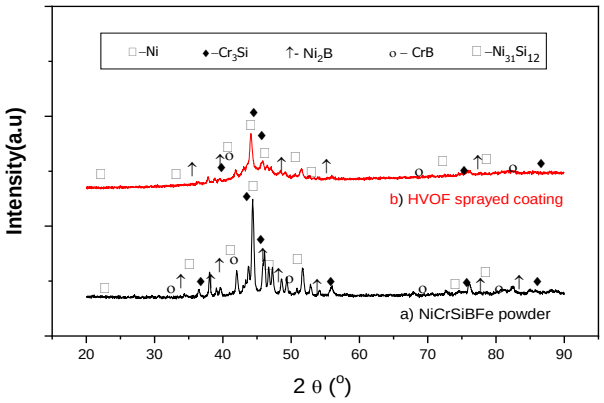

Fig. 1. XRD graph of powder and coating.

Nickel-based solid-solution found as the key-phase in the coating owing to the base elements in the feedstock powder. The silicates and boride crystals have observed on the coating surface. The high and sharp peaks confirm the crystalline phases at a certain position. Similar phases have been reported in the literature by [24,32]. The coating thickness was found to vary from 214 to 294 µm, as shown in the cross-section image in Figs. 2 and 3 shows the as-sprayed surface SEM micrographs and the various elements exist in the coating surface at a different position. The melted particles, spherical nodules with small pores, were observed on the coating surface. The coating porosity was measured 0.74± 0.18 %. The nano-hardness and the effective elasticity modulus of the coating were 7.14± 0.85 GPa and 149±16 GPa, respectively.

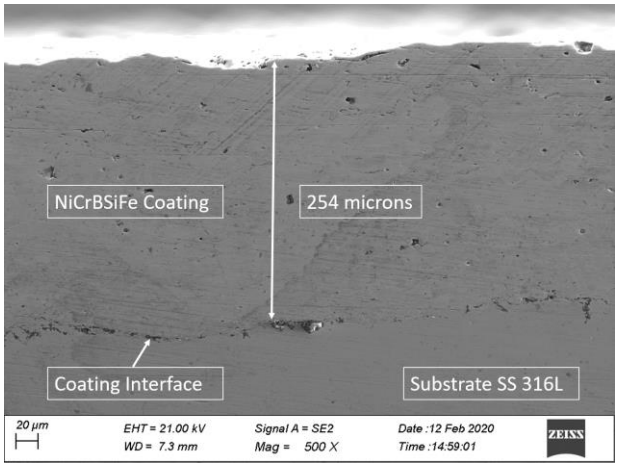

Fig. 2. HVOF sprayed coating cross section [33].

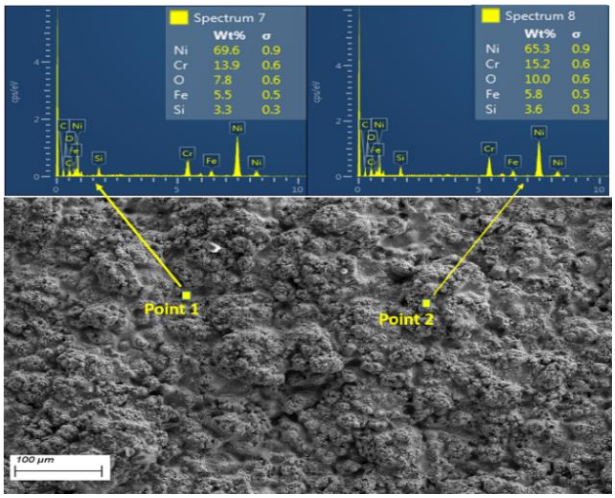

Fig. 3. SEM and EDX of As-sprayed coating surface.

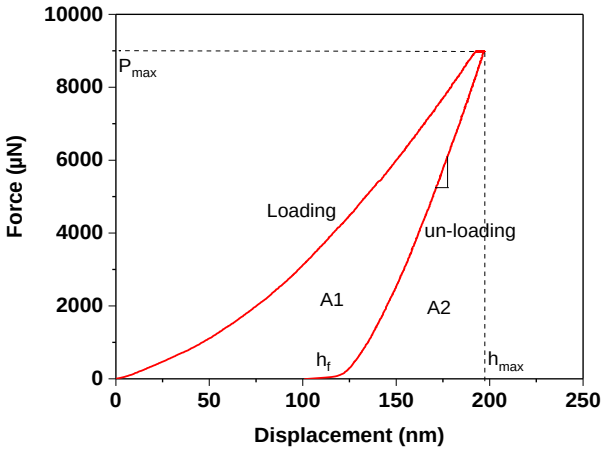

Fig. 4. Loading and un-loading curve for nano-indentation

Table 2. Properties of the coatings.

The effective elasticity modulus (Er, GPa)	Hardness (H, GPa)	H/E_r	Yield pressure (H^3/E_r^2, GPa)	Elastic recovery η (%)	As-sprayed roughness (Ra, μm)	Porosity (%)	Thickness (μm)
149±16	7.14± 0.85	0.0479	0.0163	42.01	5.87 ± 0.76	0.74± 0.18	254± 40

Figure 4 shows the loading and unloading curve for the nano-indentation performed on the coating cross-section at 150 μm depth from the surface.

The area under the unloading curve represents the elastic energy as denoted by A_2. The ratio of the elastic energy (A_2) and the total deformation energy (A_1+A_2) indicates the elastic recovery value (η). The HVOF sprayed coating has higher hardness than the plasma sprayed, and spray-fused NiCrBSi powder coating, due to the better adhesion and the flawless spreading of the precipitate [22]. Table 2 shows the properties of HVOF sprayed NiCrBSiFe coating. The nano-hardness, H/E_r ratio, the elastic recovery (η), porosity and as-sprayed roughness values in the Table 2, indicate that the HVOF process produces a better deposition than the FS-flame and FS-laser processes used in the literature [18].

3.2 The co-efficient of friction and wear-track microstructure

The coefficient of friction was plotted against the sliding distance as obtained from the various test condition. It is observed that, with increasing temperature from 300 °C to 700 °C the coefficient of friction increases, and maximum at room temperature condition. Figure 5 shows the COF variation over 0 to 1800 m sliding distance for the coating against silicon nitride material at various temperature condition. The coefficient of friction variation found uniform throughout the sliding wear time for room temperature, 300 and 700 °C. At 500 °C temperature the COF changes suddenly at 800 m sliding distance from 0.1 to 0.5. These results were comparable to the results obtained in the literature by Shaikh asad ali dilawary et al. [34]. The author has plotted the COF for NiCrBSi powder coated by hard-facing method at elevated temperatures up to 700 °C for 500 m sliding distance and compared with the results obtained for NiCrBSi + 10 wt.% Mo hard-facings. Chun Guo et al. [35], concluded that when sliding of Si_3N_4 counter material take place with stainless steel at 500 °C, there exist severe plastic deformation, adhesion, abrasion and cutting wear mechanism. From the observation during the experimentation, there was a sudden rise in the vibration and sound level after 800 m sliding distance. From the temperature range 0 – 500 °C, no significant change in the hardness of the coating occurred, but when the temperature increases further, there is a rapid reduction in the hardness of the coating [27]. The oxide layer prevents the direct contact between the coatings, and counter body resulting in reducing the coefficient of friction.

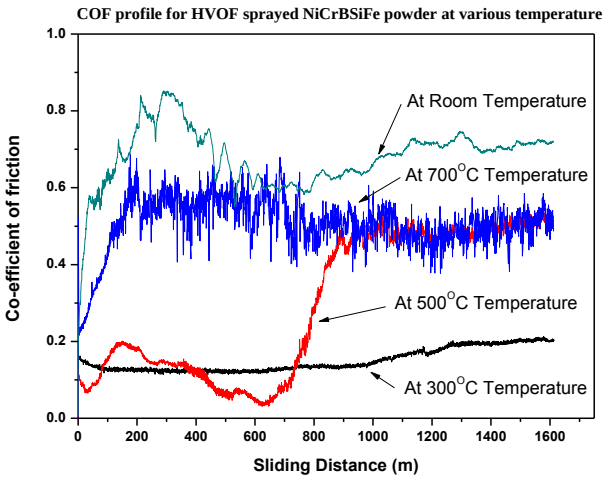

Fig. 5. Coefficient of friction profile of coating.

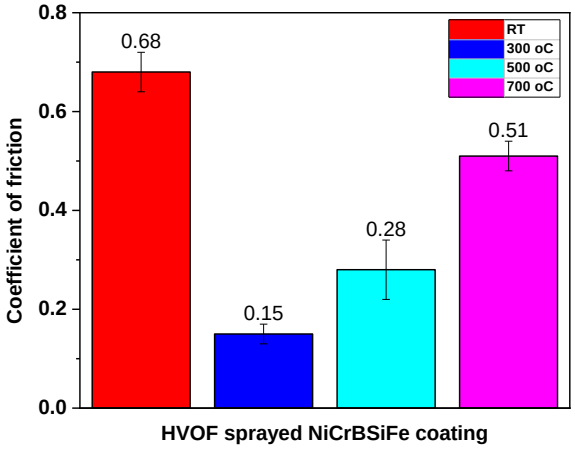

Fig. 6. Coefficient of friction for HVOF sprayed coating at different temperature.

Zhou, W et al. [26] reported similar observation for the HVOF sprayed Cr_3C_2-NiCr coatings against alumina. The coefficient of friction increases with the temperature, due to higher oxide formation and oxide removal due to sliding on the surface. The oxide act as third particles in the contact and hence increases the COF. Matteo Federici et al. [13] concluded that wide and thick layer formed on the surface from the commencement of the test at 300 °C due to thermal softening, and the COF remains constant throughout the experiment. The results obtained for HVOF sprayed coating at 300 °C agreed with this conclusion. Figure 6 shows the frictional coefficients at different temperature. The temperature affects the wear damage significantly, due to oxide generation, retention and softening of the surface. The partially oxidized debris particle retains on the contacting surface. Due to sliding action, the oxide particles agglomerated, compacted and form a protective layer on the surface. The loosely compact particles are present in the layer at low temperature up to 200 °C, but at a higher temperature, the hard and protective layer developed due to increased rate of generation and retention of the particle, facilitation of compaction, sintering and oxidation [36]. The wear is influence by the oxidation, the abrasion wear, and the high-temperature mechanical properties of the Cr_3C_2-NiCr coating [28,37]. Figure 7 to 10 shows the SEM micrographs of wear tracks generated at room temperature to 700 °C temperature wear test for the coating. The abrasive wear phenomenon noticed for the coating surface at room temperature condition. The severe abrasive marks, craters and ploughing marks were observed on the wear-tracks. Due to the severe abrasive wear and the high amount of material removal, a higher wear rate was obtained, at room temperature condition. A similar wear mechanism identified from the micrographs and reported in the literature by [38,39]. At 300 °C, a small wear-track with little oxides were noticed. More oxide clusters observed on the wear-track correspond to the 500 °C condition. At 700 °C, comparatively smooth wear-track with oxide debris, and small micro-cracks were noticed. As observed from the micrograph, the microstructure of the coating governs the wear performance at the low-temperature condition. At 300 °C temperature condition, the smooth wear-track over the coating reflects the mild wear. At high-temperature, wear is influenced by the oxide layer formed and thermal softening of the coating. At 700 °C, the wear-track found fully covered with the compacted oxide layers and debris particle. A similar observation has been done by Leandro J. da Silva et al. [40] in evaluating the dilution effect on the microstructure and wears at high temperature for NiCrSiBC coatings by plasma method on a stainless steel substrate.

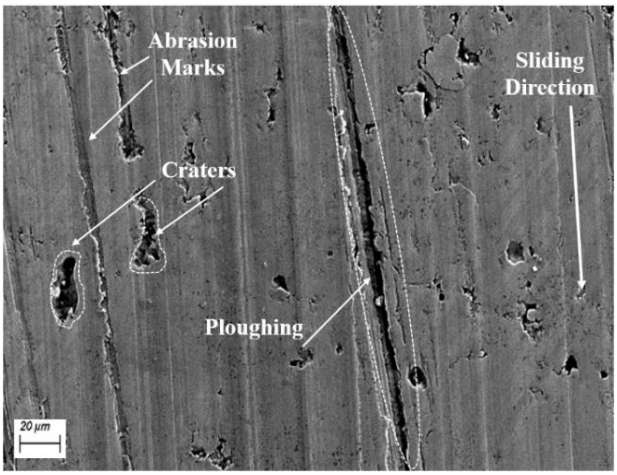

Fig. 7. The wear-track SEM micrograph at room temperature.

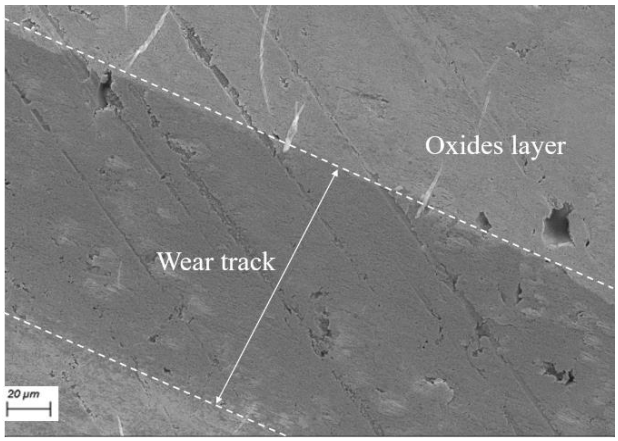

Fig. 8. The wear-track SEM micrograph at 300 °C.

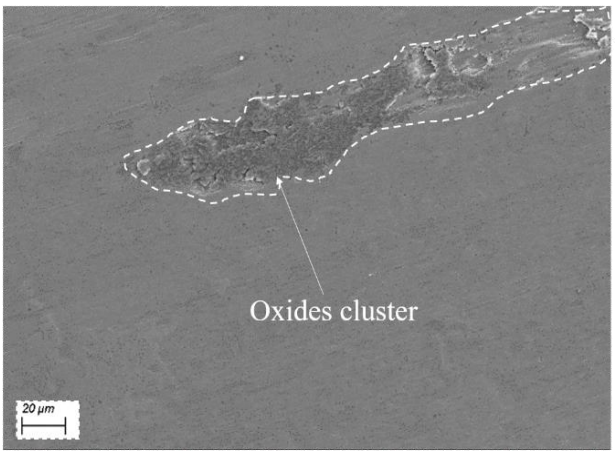

Fig. 9. The wear-track SEM micrograph at 500 °C.

Table 3 shows the elements weight percentage perceived at coating wear track. It is observed from the oxygen weight percentage that, the oxides formed during the sliding wear experiment at 300 °C are minimum, as compared to the condition at 500 °C and 700 °C.

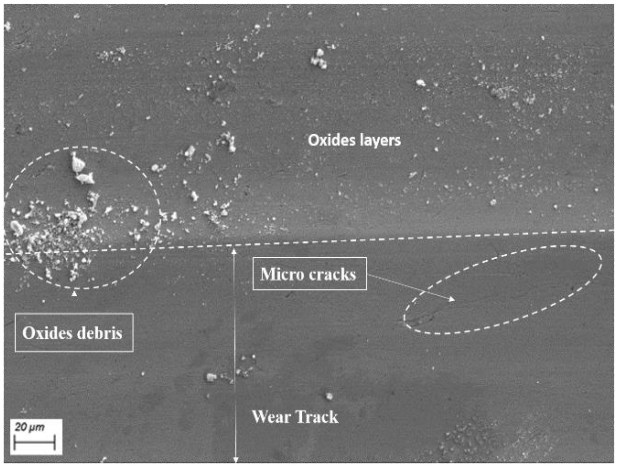

Fig. 10. The wear-track SEM micrograph at 700 °C.

Table 3. The quantitative chemical analysis.

Element	300 °C (%wt.)	500 °C (%wt.)	700 °C (% wt.)
O	0.74	1.22	2.92
Si	4.77	5.03	4.12
Cr	15.35	13.99	15.16
Fe	3.80	3.67	4.20
Ni	76.07	76.09	73.60

The more oxidation and thermal softening occurred at 700 °C as compared to 500 °C condition. The sliding wear is highly influenced by the oxidation and thermal softening of the coating at high-temperature.

3.3 3D non-contact analysis of track

The 3D wear-track profile obtained for HVOF coating sample at room temperature and 300 °C is shown in Figs. 11 and 12**.** The wear-track depth is displayed by the colour contour. The wear-track profile obtained at 500 °C and 700 °C is shown in Figs. 13 and 14. Due to the oxide particles on the wear-track, few peaks were observed in the track profile. The maximum wear-track width and depth in the wear-track were used to determine the volumetric loss of the coating material, which in term gives the specific wear rate.

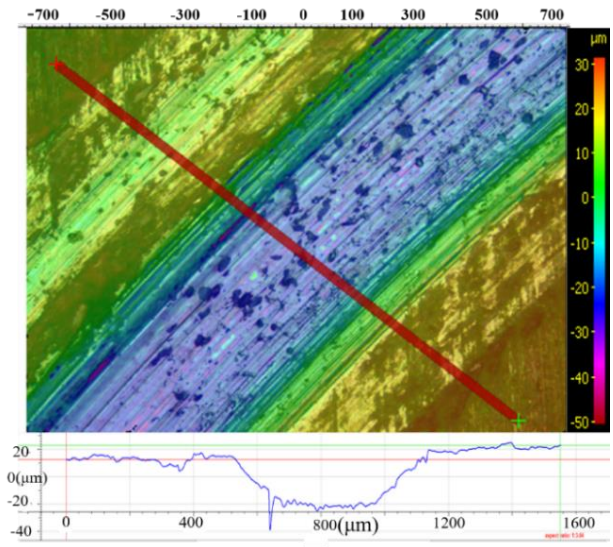

Fig. 11. The wear-track profile of coating at room temperature.

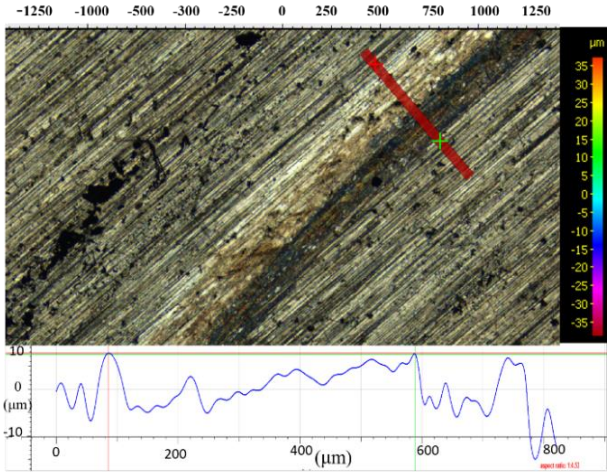

Fig. 12. The wear-track profile of coating at 300 °C.

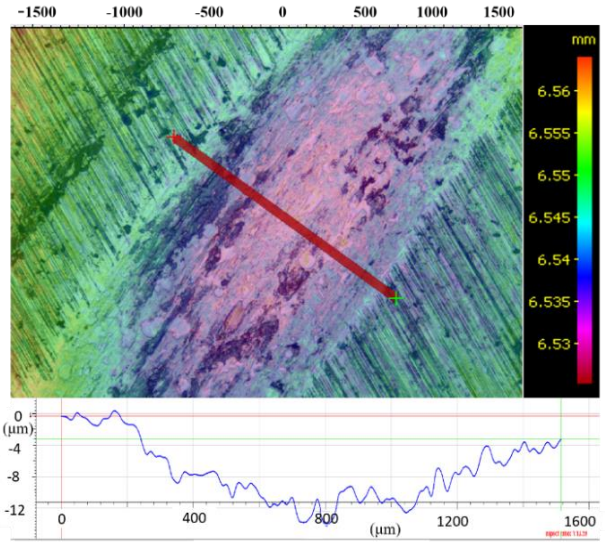

Fig. 13. The wear-track profile of coating at 500 °C.

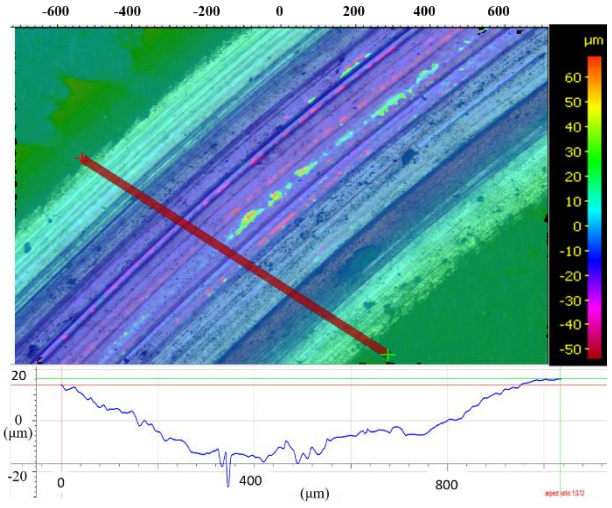

Fig. 14. The wear-track profile of coating at 700 °C.

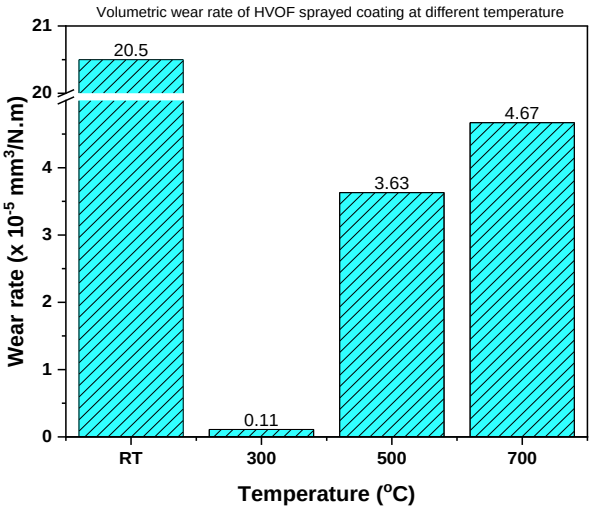

Fig. 15. The volumetric wear rate of coating at different temperature conditions.

The volumetric wear rate for the coating at dissimilar temperature is presented in Fig. 15. The wear rate for the coating found as thirty-three times and forty-two times more at 500 °C and 700 °C, respectively than at 300 °C. The least wear rate was recorded at 300 °C and the maximum wear rate at room temperature condition. The wear rate increases with the rise in temperature from 300 °C to 700 °C. At 300 °C, the stable oxide layers formed during the wear tests acted as a solid lubricant and reduced direct contact between the mating surfaces. The reduced contact area decreased the wear rate and the frictional coefficient [12,41,42]. The severe abrasion at room temperature condition changes to mild abrasive wear and very less material loss occurred from the surface, hence the minimum wear rate obtained for the coating at 300 °C. The amount of oxidation and retention of oxide layers on the surface at different temperature varies with the temperature condition. The temperature is insufficient to cause thermal softening of the coating and the oxidative damage. The oxide scale damage of the coating starts above the 500 °C as per literature.

At 500 °C and 700 °C, the breakage of the oxide phases on the surface occurred due to more thermal softening and the oxide fragmentation, which encourages the tree body abrasion at the contact. At higher temperatures, the oxide layer becomes thicker with time and cracking occurred, which give rise to more sites for adhesive wear. The surface is repeatedly exposed to oxidation. The adhering incapability of the oxide layer led to higher wear rates. Moreover, the hard and brittle oxide layer debris promotes three-body abrasive wear. These oxidative and abrasive phenomenon increases the specific wear rate and coefficient of friction as compared to the 300 °C condition. Similar observations had been reported by researchers [38,43]. The coating wear performance in unidirectional sliding wear at high temperature up to 700 °C is better than at room temperature condition. The specific wear rates of the coating, at all the temperature conditions, were varied from 10^{-7} to 10^{-4} $mm^3/N.m$, which is the mild wear range [44], indicates that the coating is serviceable up to 700 °C temperature. The higher specific wear rate and coefficient of friction at 700 °C condition are due to more oxide layer disintegration, and abrasive wear occurred at high temperature as compared to 500 °C.

3.4 Phase assessment

The phase identification has carried out to assess the transformation of the phases at different temperatures. The Raman spectrum for the wear-track at 300, 500 and 700 °C are shown in Figs. 16 and 17. The major phases were CrO_2, SiO_2, NiO and Fe_2O_3. At 300 °C temperature, the Fe_2O_3 was detected inside and outside of the wear-track surface.

At 500 °C and 700 °C, the various phases existing on the wear-track were nickel oxide (NiO), silicon oxide (SiO_2), and chromium oxide (CrO_3). These oxide phases exist at high temperature for the off-track and on-track of the surfaces indicates the oxidation of the coating and oxide formation. The noticeable high peaks observed for CrO_3 phase at 700 °C condition. The Cr, Ni and Si components of the coating do not oxidize at 300 °C and hence, not

observed in the Raman spectrum either outside the track or inside the track.

But at 500 °C and 700 °C condition, due to the oxidation occurrence, all the oxide phases have existed. For the Raman spectrum obtained for the wear track, the phases were identified by matching the Raman band for the observed peaks in the literature [45–49].

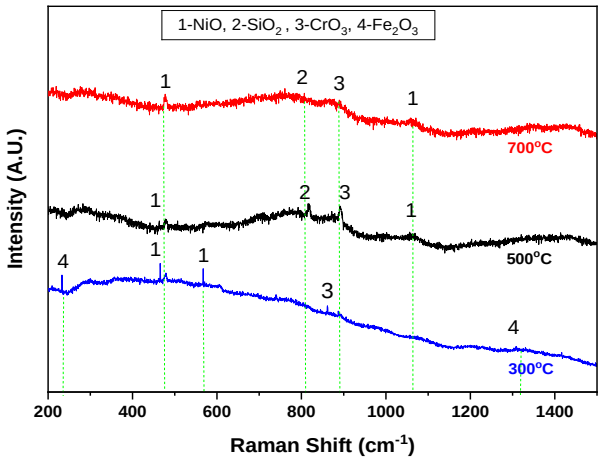

Fig. 16. Raman spectrum for off- track position of HVOF coating at various temperature.

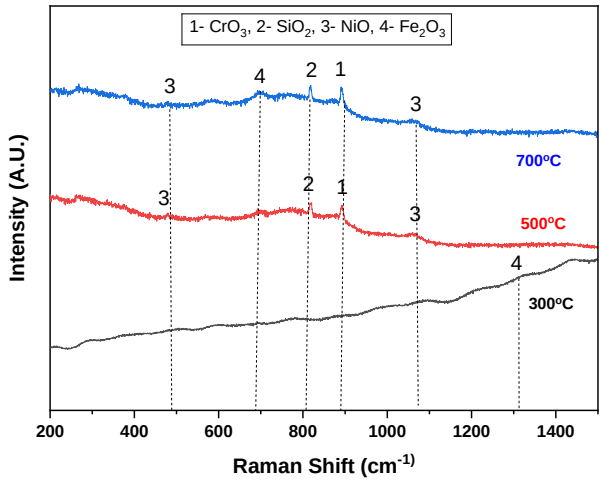

Fig. 17. Raman spectrum for on- track position of HVOF coating at various temperature.

The sharp peak wave number 900 cm^{-1} corresponds to the chromium oxide (CrO_3), and 800 cm^{-1} due to silica (SiO_2) matches with literature by M.A. Vuurman [45]. Two bands correspond to NiO at 500 cm^{-1}, and 1100 cm^{-1} with small peaks have agreed with the reference [46,49]. At 300 °C temperature, Fe_2O_3 phase observed at 1300 cm^{-1} but wiped out at 500 °C and 700 °C, the Fe_2O_3 phase has matched with reference [48]. In the SEM micrographs, some of the oxide clusters have seen inside and outside of the coating wear track. At elevated temperature, the coating wear rate affected due to the simultaneously occurring oxidation, oxide removal due to sliding and change in the hardness due to thermal softening. At 500 °C and 700 °C, the sharp peak corresponding to the retained CrO_3 phase has identified on the wear track. The broad peaks at 500 cm^{-1} and 1100 cm^{-1} indicates the retained NiO phase on the wear-track surface. The phase Fe_2O_3 has wiped out from the worn-out surface at 700 °C.

4. CONCLUSION

The high-velocity oxy-fuel sprayed NiCrBSiFe coating has investigated for friction and sliding wear behaviour at room temperature, 300, 500 and 700 °C. The main findings can be summarized as follows:

- The HVOF process produces highly dense, crack-free, low porous and high hardness coating of NiCrBSiFe on stainless steel 316L substrate.
- The highest specific wear rate and COF at room temperature reduced drastically at 300 °C temperature. The wear rate at 500 °C and 700 °C, found thirty-three and forty-two times the wear rate at 300 °C. At 300 °C, the least specific wear rate and COF are owing to the thermal softening and lubricious oxide layer formation on the coating.
- At 700 °C, the substantial amount of material loss from the coating surface occurred due to the fatigue delamination, thermal softening and oxide fragmentation during sliding.
- The wear phenomena change to a combination of oxidation and abrasive at high-temperature from the severe abrasion at room temperature condition.
- The specific wear rates of the coating in the mild wear range confirms the functionality of the HVOF coated components up to 700 °C.

Acknowledgement

The authors are grateful to IIT Bombay, India, for providing the testing facilities such as SEM, EDX, XRD, nano-indentation and non-contact

profilometer. The authors thank the mechanical engineering department, VJTI, Mumbai for providing support in carrying out this work. This research work did not receive any specific grant from funding agencies in the public, commercial, or not-for-profit sectors.

REFERENCES

[1] J.-K. Xiao, Y.-Q. Wu, W. Zhang, J. Chen, X.-L. Wei, C. Zhang, *Microstructure, wear and corrosion behaviors of plasma sprayed NiCrBSi-Zr coating*, Surface and Coatings Technology, vol. 360, pp. 172-180, 2019, doi: 10.1016/J.SURFCOAT.2018.12.114

[2] S. Rukhande, W.S. Rathod, D. Bhosale, *Tribological Behaviour of Thermally Sprayed Coatings : A Review*, in An International Conference on Tribology, 13-15 December, 2018, TRIBOINDIA-2018, VJTI, Mumbai, SSRN, pp. 13–16, doi: 10.2139/ssrn.3323697

[3] F. Otsubo, H. Era, K. Kishitake, *Structure and phases in nickel-base self-fluxing alloy coating containing high chromium and boron*, Journal of Thermal Spray Technology, vol. 9, pp. 107–113, 2000, doi: 10.1361/10599630077 0350131

[4] M.A. Garrido, A. Rico, M.T. Gómez, M. Cadenas, J.E. Fernández-Rico, J. Rodríguez, *Tribological and Oxidative Behavior of Thermally Sprayed NiCrBSi Coatings*, Journal of Thermal Spray Technology, vol. 26, pp. 517-529, 2017, doi: 10.1007/s11666-016-0521-6

[5] U. Heubner, H. Alves, *Aqueous corrosion of Nickel and its alloys*, Shreir's Corrosion, vol. 3, pp. 1916–1936, 2010, doi: 10.1016/B978-044452787-5.00093-7

[6] Š. Houdková, E. Smazalová, M. Vostřák, J. Schubert, *Properties of NiCrBSi coating, as sprayed and remelted by different technologies*, Surface and Coatings Technology, vol. 253, pp. 14–26, 2014, doi: 10.1016/j.surfcoat.2014.05. 009

[7] B. Yin, G. Liu, H. Zhou, J. Chen, F. Yan, *Sliding wear behavior of HVOF-sprayed Cr3C2-NiCr/CeO2 composite coatings at elevated temperature up to 800 °C*, Tribology Letters, vol. 37, pp. 463-475, 2010, doi: 10.1007 /s11249-009-9540-5

[8] P.C. Yu, X.B. Liu, X.L. Lu, S.J. Qiao, Y.J. Zhai, G.X. Zhu, Y.G. Wang, Y. Chen, *Tribology and high-temperature oxidation behaviors of NiCrBSiFe composite coatings on Ti6Al4V alloy by laser cladding*, RSC Advances, iss. 93, pp. 76516-76525, 2015, doi: 10.1039/c5ra14732 h

[9] D. Chaliampalias, G. Vourlias, E. Pavlidou, S. Skolianos, K. Chrissafis, G. Stergioudis, *Comparative examination of the microstructure and high temperature oxidation performance of NiCrBSi flame sprayed and pack cementation coatings*, Applied Surface Science, vol. 255, iss. 6, pp. 3605-3612, 2009, doi: 10.1016/j.apsusc. 2008.10.006

[10] N.L. Parthasarathi, M. Duraiselvam, U. Borah, *Effect of plasma spraying parameter on wear resistance of NiCrBSiCFe plasma coatings on austenitic stainless steel at elevated temperatures at various loads*, Materials & Design, vol. 36, pp. 141-151, 2012, doi: 10.1016/j.matdes.2011.10.051

[11] E.E. Anand, S. Natarajan, *High-temperature erosion behaviour of plasma-sprayed NiCrBSi–graphite coatings*, Surface Engineering, vol. 34, iss. 10, pp. 783-790, 2018, doi: 10.1080/02670844.2018.1467143

[12] S. Dong, B. Song, H. Liao, C. Coddet, *Deposition of NiCrBSi coatings by atmospheric plasma spraying and dry-ice blasting: Microstructure and wear resistance*, Surface and Coatings Technology, vol. 268, pp. 36-45, 2015, doi: 10.1016/j.surfcoat.2014.09.025

[13] M. Federici, C. Menapace, A. Moscatelli, S. Gialanella, G. Straffelini, *Pin-on-disc study of a friction material dry sliding against HVOF coated discs at room temperature and 300 °C*, Tribology International, vol. 115, pp. 89-99, 2017, doi: 10.1016/j.triboint.2017.05.030

[14] D.G. Bhosale, W.S. Rathod, S.W. Rukhande, *Sliding wear behavior of high velocity oxy-fuel sprayed WC-Cr3C2-Ni coating for automotive applications*, Materialstoday: Proceedings, vol. 19, iss. 2, pp. 339-343, 2019, doi: 10.1016/j.matpr.2019.07.609

[15] S.W. Rukhande, W.S. Rathod, *Tribological Behaviour of Plasma and HVOF sprayed NiCrSiBFe Coatings*, Surface Engineering, vol. 36, iss. 7, pp. 745-755, 2020, doi: 10.1080/02670844.2020.1730062

[16] H. Vasudev, L. Thakur, A. Bansal, H. Singh, S. Zafar, *High temperature oxidation and erosion behaviour of HVOF sprayed bi-layer Alloy-718/NiCrAlY coating*, Surface and Coatings Technology, vol. 362, pp. 366-380, 2019, doi: 10.1016/j.surfcoat.2019.02.012

[17] V.H. Hidalgo, F.J.B. Varela, A.C. Menéndez, S.P. Martínez, *A comparative study of high-temperature erosion wear of plasma-sprayed NiCrBSiFe and WC-NiCrBSiFe coatings under simulated coal-fired boiler conditions*, Tribology International, vol. 34, iss. 3, pp, 161-169, 2001, doi: 10.1016/S0301-679X(00)0014 6-8

[18] T. Gómez-del Río, M.A. Garrido, J.E. Fernández, M. Cadenas, J. Rodríguez, *Influence of the deposition techniques on the mechanical properties and microstructure of NiCrBSi coatings*, Journal of Materials Processing Technology, vol. 204, iss. 1-3, pp. 304-312, 2008, doi: 10.1016/j.jmatprotec.2007.11.042

[19] B. Yin, H.D. Zhou, J.M. Chen, F.Y. Yan, *Microstructure and high temperature sliding wear behaviour of laser remelted NiCrBSi/35(WC-12Ni) composite coating*, Surface Engineering, vol. 27, iss. 6, pp. 458-463, 2011, doi: 10.1179/026708410X1268735 6948517

[20] D.G. Bhosale, W.S. Rathod, U.S. Ghorpade, S.W. Rukhande, *Nickel alloy C-263 protection by WC-Cr3C2-Ni coatings against high-temperature wear in nuclear applications, Surfaces and Interfaces*, vol. 21, 2020, doi: 10.1016/j.surfin.2020.100689

[21] H. Vasudev, L. Thakur, H. Singh, A. Bansal, *An investigation on oxidation behaviour of high velocity oxy-fuel sprayed Inconel718-Al2O3 composite coatings*, Surface and Coatings Technology, vol. 393, 2020, doi: 10.1016/j.surfcoat.2020.125770

[22] J.M. Miguel, J.M. Guilemany, S. Vizcaino, *Tribological study of NiCrBSi coating obtained by different processes*, Tribology International, vol. 36, iss. 3, pp. 181-187, 2003, doi: 10.1016/S0301-679X(02)00144-5

[23] D. Kong, B. Zhao, *Effects of loads on friction–wear properties of HVOF sprayed NiCrBSi alloy coatings by laser remelting*, Journal of Alloys and Compounds, vol. 705, pp. 700-707, 2017, doi: 10.1016/j.jallcom.2017.02.171

[24] G. Singh, M. Kaur, R. Upadhyaya, *Wear and Friction Behavior of NiCrBSi Coatings at Elevated Temperatures*, Journal of Thermal Spray Technology, vol. 28, pp. 1081–1102, 2009, doi: 10.1007/s11666-019-00876-y

[25] G. Singh, M. Kaur, *High-temperature wear behaviour of HVOF sprayed 65% (NiCrSiFeBC)–35% (WC–Co) coating*, Surface Engineering, vol. 36, iss. 11, pp. 1139-1155, 2020, doi: 10.1080/02670844.2019.1639932

[26] W. Zhou, K. Zhou, Y. Li, C. Deng, K. Zeng, *High temperature wear performance of HVOF-sprayed Cr3C2 -WC-NiCoCrMo and Cr3C2-NiCr hardmetal coatings*, Applied Surface Science, vol. 416, pp. 33-44, 2017, doi: 10.1016/j.apsusc.2017.04.132

[27] A. Zikin, M. Antonov, I. Hussainova, L. Katona, A. Gavrilović, *High temperature wear of cermet particle reinforced NiCrBSi hardfacings*, Tribology International, vol. 68, pp. 45-55, 2013, doi: 10.1016/j.triboint.2012.08.013

[28] H. Wu, D. Kong, *Effects of laser power on friction–wear performances of laser thermal sprayed Cr3C2-NiCr composite coatings at elevated temperatures*, Optics & Laser Technology, vol. 117, pp. 227–238, 2019, doi: 10.1016/j.optlastec.2019.04.022

[29] P.R. Reinaldo, A.S.C.M. D'Oliveira, *NiCrSiB coatings deposited by plasma transferred arc on different steel substrates*, Journal of Materials Engineering and Performance, vol. 22, pp. 590–597, 2013, doi: 10.1007/s11665-012-0271-7

[30] J. Musil, F. Kunc, H. Zeman, H. Poláková, *Relationships between hardness, Young's modulus and elastic recovery in hard nanocomposite coatings*, Surface and Coatings Technology, vol. 154, iss. 2-3, pp. 304–313, 2002, doi: 10.1016/S0257-8972(01)01714-5

[31] J.B. Cheng, X.B. Liang, B.S. Xu, *Devitrification of arc-sprayed FeBSiNb amorphous coatings: Effects on wear resistance and mechanical behavior*, Surface and Coatings Technology, vol. 235, pp. 720–726, 2013, doi: 10.1016/j.surfcoat.2013.08.054

[32] W. Zórawski, S.J. Skrzypek, *Tribological properties of plasma and HVOF-sprayed NiCrBSi-Fe2O3 composite coatings*, Surface and Coatings Technology, vol. 220, pp. 282–289, 2013, doi: 10.1016/j.surfcoat.2012.09.057

[33] S.W. Rukhande, W.S. Rathod, *An isothermal oxidation behaviour of atmospheric plasma and high-velocity oxy-fuel sprayed nickel based coating*, Ceramics International, vol. 46, iss. 11, B, pp. 18498–18506, 2020, doi: 10.1016/j.ceramint.2020.04.155

[34] S.A.A. Dilawary, A. Motallebzadeh, E. Atar, H. Cimenoglu, *Influence of Mo on the high temperature wear performance of NiCrBSi hardfacings*, Tribology International, vol. 127, pp. 288–295, 2018, doi: 10.1016/j.triboint.2018.06.022

[35] C. Guo, J. Zhou, J. Chen, J. Zhao, Y. Yu, H. Zhou, *High temperature wear resistance of laser cladding NiCrBSi and NiCrBSi/WC-Ni composite coatings*, Wear, vol. 270, iss. 7-8, pp. 492–498, 2011, doi: 10.1016/j.wear.2011.01.003

[36] F.H. Stott, *High-temperature sliding wear of metals*, Tribololgy International, vol. 35, iss. 8, pp. 489–495, 2002, doi: 10.1016/S0301-679X(02)00041-5

[37] H. Wang, X. Yan, H. Zhang, M. Gee, C. Zhao, X. Liu, *Oxidation-dominated wear behaviors of carbide-based cermets : A comparison between WC-WB-Co and Cr3C2-NiCr coatings*, Ceramics International, vol. 45, iss. 17, A, pp. 21293–21307, 2019, doi: 10.1016/j.ceramint.2019.07. 113

[38] G. Bolelli, L.-M. Berger, T. Börner, H. Koivuluoto, V. Matikainen, L. Lusvarghi, C. Lyphout, N. Markocsan, P. Nylén, P. Sassatelli, R. Trache, P. Vuoristo, *Sliding and abrasive wear behaviour of HVOF- and HVAF-sprayed Cr3C2-NiCr hardmetal coatings*, Wear, vol. 358–359, pp. 32–50, 2016, doi: 10.1016/j.wear.2016.03.034

[39] S.W. Rukhande, W.S. Rathod, D.G. Bhosale, *Dry sliding wear behaviour of HVOF sprayed NiCrBSiFe coating on SS 316L*, Materialstoday: Proceedings, In Press, 2020, doi: 10.1016/j.matpr.2020. 08.408

[40] L.J. da Silva, A.S.C.M. D'Oliveira, *NiCrSiBC coatings: Effect of dilution on microstructure and high temperature tribological behavior*, Wear, vol. 350–351, pp. 130–140, 2016, doi: 10.1016/j.wear.2016.01.015

[41] L. Liu, H. Xu, J. Xiao, X. Wei, G. Zhang, C. Zhang, *Effect of heat treatment on structure and property evolutions of atmospheric plasma sprayed NiCrBSi coatings*, Surface and Coatings Technology, vol. 325, pp. 548–554, 2017, doi: 10.1016/j.surfcoat.2017.07.011

[42] T.B. Torgerson, M.D. Harris, S.A. Alidokht, T.W. Scharf, S.M. Aouadi, R.R. Chromik, J.S. Zabinski, A.A. Voevodin, *Room and elevated temperature sliding wear behavior of cold sprayed Ni-WC composite coatings*, Surface and Coatings Technology, vol. 350, pp. 136-145, 2018, doi: 10.1016/j.surfcoat.2018.05.090

[43] J. Hardell, B. Prakash, *Tribological performance of surface engineered tool steel at elevated temperatures*, International Journal of Refractory Metals and Hard Materials, vol. 28, iss. 1, pp. 106–114, 2010, doi: 10.1016/j.ijrmhm.2009.07.009

[44] K. Kato, *Friction and wear of passive metals and coatings*, Tribocorrosion of Passive Metals and Coatings. Woodhead Publishing Series in Metals and Surface Engineering, pp. 65–97, 2011, doi: 10.1533/9780857093738.1.65

[45] M.A. Vuurman, I.E. Wachs, D.J. Stufkens, A. Oskam, *Characterization of chromium oxide supported on Al2O3, ZrO2, TiO2, and SiO2 under dehydrated conditions*, Journal of Molecular Catalysis, vol. 80, iss. 2, pp. 209–227, 1993, doi: 10.1016/0304-5102(93)85079-9

[46] N. Mironova-Ulmane, A. Kuzmin, I. Steins, J. Grabis, I. Sildos, M. Pärs, *Raman scattering in nanosized nickel oxide*, Journal of Physics: Conference Series, vol. 93, pp. 1–7, 2007, doi: 10.1088/1742-6596/93/1/012039

[47] Y. El Mendili, J.-F. Bardeau, N. Randrianantoandro, A. Gourbil, J.-M. Greneche, A.-M. Mercier, F. Grasset, *New evidences of in situ laser irradiation effects on γ-Fe2O3 nanoparticles: A Raman spectroscopic study*, Journal of Raman Spectroscopy, vol. 42, iss. 2, pp. 239–242, 2010, doi: 10.1002/jrs.2762

[48] D.L.A. De Faria, S. Venâncio Silva, M.T. de Oliveira, *Raman microspectroscopy of some iron oxides and oxyhydroxides*, Journal of Raman Spectroscopy, vol. 28, iss. 11, pp. 873-878, 1998, doi: 10.1002/(sici)1097-4555(199711)28:11<873::aid-jrs177>3.3.co;2-2

[49] S.H. Lee, H.M. Cheong, N.G. Park, C.E. Tracy, A. Mascarenhas, D.K. Benson, S.K. Deb, *Raman spectroscopic studies of Ni-W oxide thin films*, Solid State Ionics, vol. 140, iss. 1-2, pp. 135–139, 2001, doi: 10.1016/S0167-2738(01)007 07-X